Stereotactic PET Atlas of the Human Brain: Aid for Visual Interpretation of Functional Brain Images

Satoshi Minoshima, Robert A. Koeppe, Kirk A. Frey, Makiko Ishihara and David E. Kuhl

Division of Nuclear Medicine, Department of Internal Medicine, The University of Michigan, Ann Arbor, Michigan

In the routine analysis of functional brain images obtained by PET, subjective visual interpretation is often used for anatomic localization. To enhance the accuracy and consistency of the anatomic interpretation, a PET stereotactic atlas and localization approach was designed for functional brain images. **Methods:** The PET atlas was constructed from a high-resolution [^{18}F]fluorodeoxyglucose (FDG) image set of a normal volunteer (a 41-yr-old woman). The image set was reoriented stereotactically, according to the intercommissural (anterior and posterior commissures) line and transformed to the standard stereotactic atlas coordinates. Cerebral structures were annotated on the transaxial planes by using a proportional grid system and surface-rendered images. The stereotactic localization technique was applied to image sets from patients with Alzheimer's disease, and areas of functional alteration were localized visually by referring to the PET atlas. **Results:** Major brain structures were identified on both transaxial planes and surface-rendered images. In the stereotactic system, anatomic correspondence between the PET atlas and stereotactically reoriented individual image sets of patients with Alzheimer's disease facilitated both indirect and direct localization of the cerebral structures. **Conclusion:** Because rapid stereotactic alignment methods for PET images are now available for routine use, the PET atlas will serve as an aid for visual interpretation of functional brain images in the stereotactic system. Widespread application of stereotactic localization may be used in functional brain images, not only in the research setting, but also in routine clinical situations.

Key Words: emission CT; brain atlas; stereotaxy; image interpretation; Alzheimer's disease

J Nucl Med 1994; 35:949–954

When interpreting functional signals from the brain measured by PET or SPECT, the anatomic localization is indispensable. This can be achieved by two different approaches: direct and indirect. In direct localization, structures that can be appreciated directly by the imaging modality are identified. When applied to PET images, this approach is limited to certain areas of the brain because of the relatively low spatial resolution of PET. In indirect localization, cerebral structures are identified by referring either to individual anatomic maps or to a standard reference system. In the first approach, PET signals can be localized by comparison with individual anatomic images of the same subject. MRI and CT can serve this purpose, although the PET and anatomic image sets need to be aligned precisely in the same orientation. In the latter approach, PET images are oriented in a standard coordinate system in which the locations of brain structures are predefined.

The orbitomeatal (OM) line, a well-known landmark for brain imaging, is one example of a reference for indirect localization. The OM line can be approximated for each subject prior to scanning, and the locations of various brain structures in this orientation are fairly consistent. Brain atlases based on the OM line have been reported to help in the interpretation of x-ray tomographic brain images (*1,2*). However, because the OM line is determined from bony landmarks of the skull, individual variations inherent in the spatial relationships between skulls and brains can cause localization errors and limit accuracy (*3*). Landmarks determined within the brain, however, should provide a more consistent orientation for brain imaging.

The intercommissural line, which passes through the anterior and posterior commissures (AC-PC), has been used for the stereotactic localization of brain structures during the past few decades (*4–6*). Applications of stereotactic localization have been described previously for CT (*7–9*) and MRI (*10–14*). Fox et al. (*15*) introduced the stereotactic method for PET images and optimized the method for [^{15}O]water studies of neuronal activation. They further developed an intersubject averaging technique for such studies, demonstrating the feasibility of stereotactic orientation (*16*). Their method for the AC-PC line determination was based on the glabella-inion line detected on a lateral skull radiograph obtained simultaneously with PET. Methods for AC-PC line estimation have been developed using PET images alone (*17,18*), which enable consistently more precise stereotactic orientation than the skull landmark determination. Although these methods were developed originally for [^{15}O] water activation studies, the stereotactic orientation was also found to be helpful for interpreting other types of PET studies (*19*).

Received Aug. 12, 1993; revision accepted Mar. 3, 1994.

For correspondence or reprints contact: Satoshi Minoshima, MD, University of Michigan Medical School, Cyclotron/PET Facility, 3480 Kresge III Bldg., Ann Arbor, MI 48109-0552.

Because PET and MRI findings from the same subject are not necessarily acquired in the same orientation in the clinical setting, the stereotactic approach is extremely helpful in reducing biases inherent in visual interpretation. Axial sampling of PET scanners has been improved recently, allowing retrospective reorientation of the images according to reliable internal reference landmarks. Bergvall et al. (*20*) predicted in their recent review that "the use of external reference systems in brain imaging should sink into oblivion—excepting only the special application of a stereotaxic frame for localization and treatment of lesions." The authors concur, expecting a broad application of the bicommissural stereotactic approach, not only in research, but also in clinical settings.

In this article, the authors present a PET stereotactic brain atlas as an aid for indirect anatomic interpretation of functional brain images in the stereotactic coordinates. No stereotactic PET atlas has yet been reported. For clinical applications of functional imaging, e.g., evaluating metabolic or perfusion patterns in dementia (*21,22*), visual interpretation of PET and SPECT images still plays an important role. The authors' intentions of presenting this PET stereotactic atlas are (1) to provide a reference atlas that has similar characteristics to functional brain images, (2) to show actual applications in Alzheimer's disease for localizing metabolic abnormalities and (3) to discuss applications and limitations of the stereotactic approach.

MATERIALS AND METHODS

Cerebral glucose metabolic image sets were obtained from 11 healthy normal volunteers. None of the volunteers had prior history of neurologic or psychiatric disorders or any major medical illness. Each subject had a normal neurologic examination on the day of PET imaging. Following intravenous injection of 370 MBq (10 mCi) of FDG, a 47-slice image set was obtained over 30 min, starting at 30 min postinjection, using a Siemens ECAT EXACT (model 921) scanner (CTI Inc., Knoxville, TN). The maximum axial and transaxial resolutions are 5 mm and 6 mm full width at half-maximum (FWHM), respectively (*23*). Tomographic images were reconstructed by using a Shepp filter with a cutoff frequency of 0.45 cycles/projection element, and the attenuation correction was estimated with an automated contour-fitting routine. The image acquisition followed a standard protocol routinely used in this laboratory.

The intercommissural (AC-PC) line was determined in each individual's image set by using the automated method previously reported (*18*). First, the midsagittal plane of the brain was determined automatically by the method described previously (*24*). Subsequently, the AC-PC line was estimated from four landmarks in the brain: the anterior pole of the brain, the most ventral aspect of the corpus callosum, the subthalamic point and the posterior pole of the brain. On the basis of the estimated midsagittal plane and the AC-PC line, the image set was transformed into stereotactic atlas coordinates. The size of the brain was corrected to the atlas's brain size by linear scaling of the anteroposterior length, height and width. This procedure takes only minutes on a common computerized workstation (SPARCstation, Sun Microsystems, Mountain View, CA).

In each normal subject, structural similarity between the Talairach and Tournoux (*25*) atlas' brain and the individual's PET image set was inspected visually, paying attention to the locations of major identifiable brain structures in the stereotactic system, such as the semsorimotor cortex. A PET image set from a 41-yr-old woman (right handed) was selected for the construction of the PET atlas. Small regional anatomic differences between the Talairach and Tournoux (*25*) atlas' brain and the selected PET brain image set were minimized by matching contours from the PET and the atlas' brains by using edge detection (*26*) and nonlinear warping techniques (modified from (*27*)). Using transformation matrices obtained through this image processing, the original PET image set, with a pixel size of 1.875 mm and a slice thickness of 3.375 mm, was transformed with a single operation and resampled with a uniform voxel size of 2.25 mm.

In the transformed image set, the right hemisphere was removed, and the left hemisphere was transposed about the midsagittal plane, creating a symmetric PET brain atlas. Proportional grids (*6,25*) were overlaid on the images to help in the anatomic localization. Major brain structures annotated on the transaxial planes were identified. When localizing cortical structures, surface-rendered images created from the transformed PET image set were also used. Each surface pixel value was determined from the highest gray matter value on a line within six pixels of and perpendicular to the surface. Anterior, posterior, superior, inferior and lateral views of the brain were formed. The right hemisphere was not removed on the rendered images to demonstrate the presence of hemispheric differences. The identification of structures on both transaxial and rendered images was accomplished by referring to stereotactic and other atlases (*6,25,28,29*). The high-resolution PET image set itself allowed the identification of major brain structures by visual inspection. When annotating structures, the abbreviations used by Talairach and Tournoux (*25*) were largely followed to facilitate easy cross-referencing.

Glucose metabolic image sets of three patients with probable Alzheimer's disease were selected randomly from the PET image database. In each patient, the diagnosis of Alzheimer's disease was based on National Institute of Neurological and Communicative Disorders and Stroke and Alzheimer's Disease and Related Disorders Association criteria. Each study was performed by using a Siemens 931/08-12 scanner (CTI) with 370 MBq (10 mCi) of FDG. Images were reconstructed with a Shepp filter with a cutoff frequency of 0.35 cycles/projection element, and attenuation was corrected with ellipse fitting, giving a reconstructed FWHM axial 7.0- to 7.5-mm and transaxial 7.0- to 8.0-mm resolutions. These image sets were reoriented to the stereotactic coordinates by using the automated procedure described previously (*18,24*). Assuming the routine use of the stereotactic alignment in the clinical setting, nonlinear warping was not performed for these cases. By referring to the PET stereotactic atlas, the authors localized metabolic abnormalities in each image set.

RESULTS

When localizing anatomic structures in a PET atlas image, two fundamentally different factors were considered in forming the PET signal: anatomic configuration and metabolic activity. These two factors are confounded by the relatively low resolution of most PET systems. High-count-rate areas could represent truly high metabolic activity and/or tightly convoluted gray matter relative to the scanner's resolution. A cerebral sulcus, in which two gray matter structures face each other closely, often shows relatively higher activity because of this resolution limitation. For example, the pre- and postcentral gyri opposed at the central sulcus

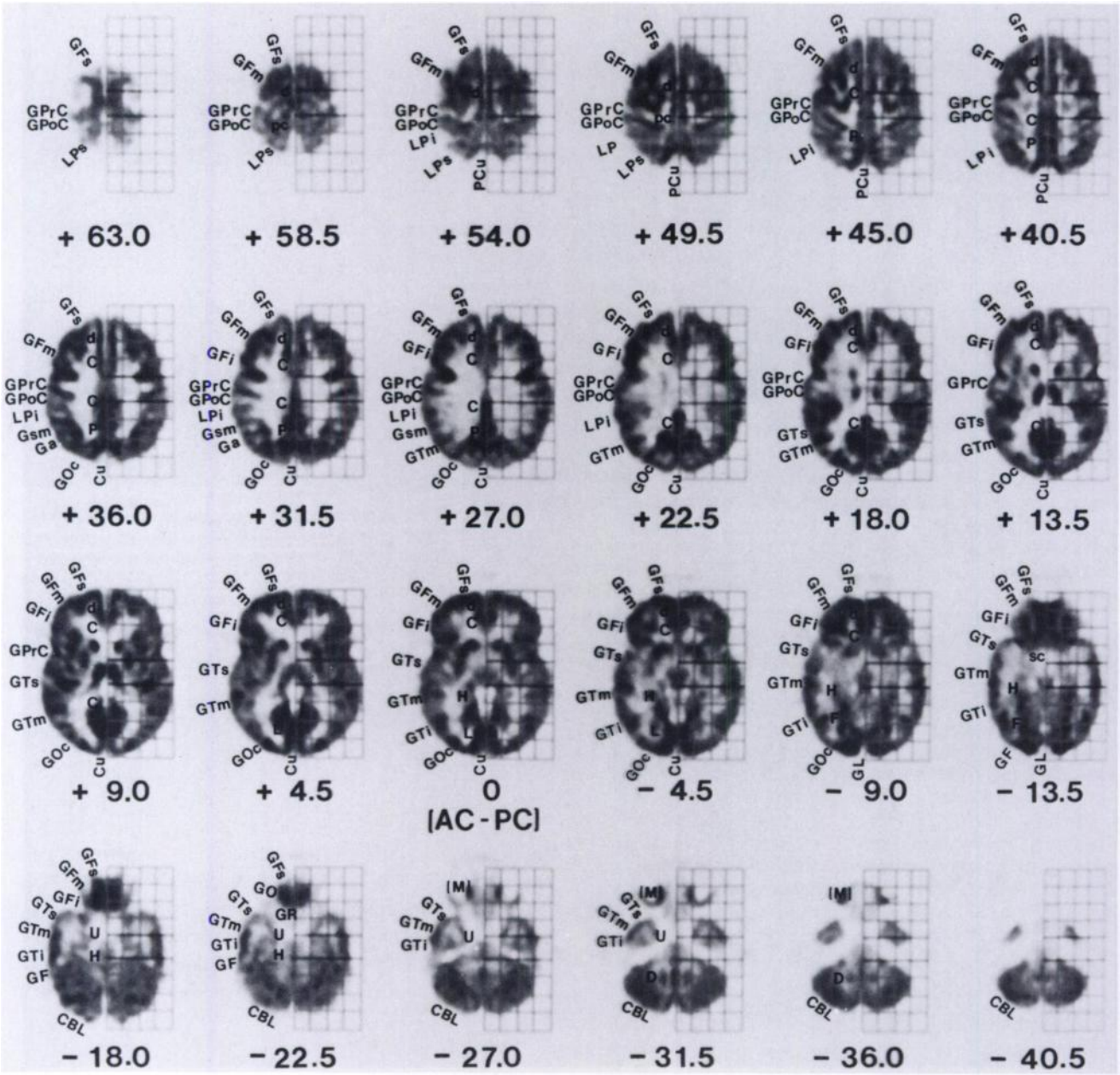

FIGURE 1. Bicommissural stereotactic brain atlas created by PET. The number on each plane represents the level (in millimeters) from the intercommissural (AC-PC) line (+ superior). Two horizontal dark lines in the proportional grids represent positions of the AC and PC (*6,24*). See Appendix for anatomic abbreviations.

cannot be distinguished by current PET scanners. Instead, the area around the sulcus forms a single focus of a relatively high activity (Fig. 1; the central sulcus is between the pre- and postcentral gyri). However, if there is a relatively large separation between two gray matter regions, e.g., medial aspects of the cerebral hemispheres in which two gray matter structures are facing but are separated by the interhemispheric fissure, these usually can be seen on a PET image as separate areas of activity (Fig. 2; two hemispheres are separated by the fissure represented as a dark line). Thus, caution must be taken when identifying cortical structures, both in tomographic and surface-rendered images.

First, major sulci and gyri were identified on the surface-rendered image (Fig. 2). Although identifiable structures are limited on the rendered images, the three-dimensional configurations of major brain structures can easily be seen. On the transverse images (Fig. 1), subcortical structures, such as the thalamus and caudate nucleus, can be localized directly. Convolutions of gyri around the precentral sulcus are distinct, separating the precentral gyrus and the other frontal gyri. The superior frontal sulcus is identified as a convolution in the frontal lobe, separating the superior and middle frontal gyri. The central sulcus has a distinct linear activity posterior to the precentral sulcus, which is located between the AC and the PC lines in the inferior slices and posterior to the PC line in the superior slices. The precen-

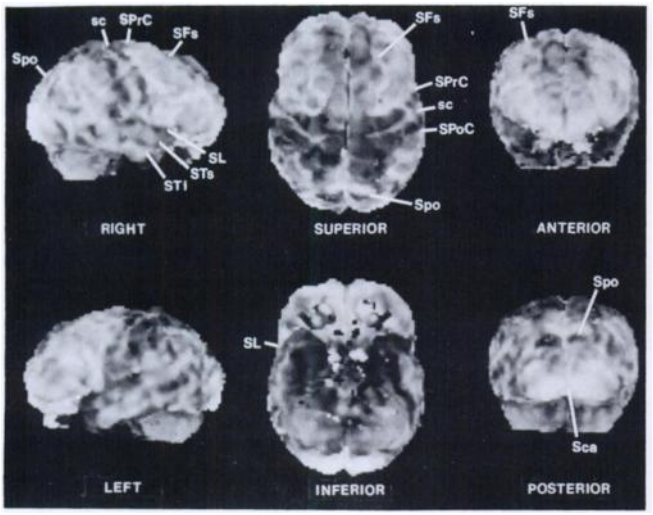

FIGURE 2. Surface-rendered images of the PET atlas. Anatomic annotations on the right hemisphere. On the superior view, the superior frontal sulcus (SFs, actually representing activity of adjacent gyri) terminates at the precentral sulcus (SPrC) by an end-to-side connection. The central sulcus (sc) is located posteriorly to the precentral sulcus on the lateral views, forming a mildly sigmoid shape in the anteroinferior to superoposterior direction. The postcentral sulcus (SPoC) is somewhat unclear. The superior and inferior temporal sulci (STs and STi) are visible on both hemispheres but more distinct on the left hemisphere. The parietooccipital sulcus (Spo) is located approximately on a line extending posteriorly from the superior temporal sulcus. The lateral sulcus (SL, sylvian fissure) shows moderate but somewhat irregular activity because of various rami and terminations of other sulci by end-to-side connections. On the lateral views (especially on the right), the ascending ramus of the sylvian fissure forms a slightly higher activity in front of the inferior end of the precentral sulcus. The inferior and intermediate frontal sulci in the frontal lobe are visible but less distinct. The angular gyrus and supramarginal gyrus are seen as areas with relatively higher activity on the lateral views; however, sulci and gyri are not completely appreciated. On the posterior view, the cuneus and lingual gyri around the calcarine sulci (Sca) show markedly high activity in this subject.

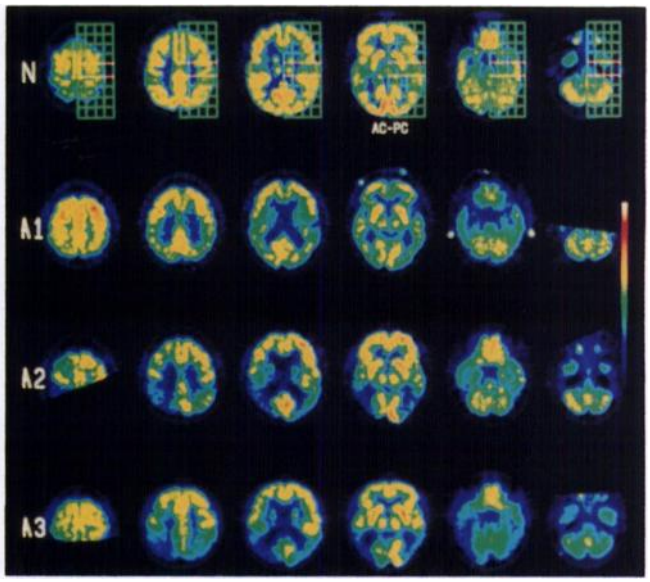

FIGURE 3. Indirect localization of functional abnormality. Three FDG PET image sets of patients with Alzheimer's disease (A1–3) were oriented to the stereotactic coordinates retrospectively and compared with corresponding planes of the normal stereotactic PET atlas (N). A1: 64-yr-old man with a clinical dementia rating (CDR) of 0.5; A2: 61-yr-old woman, CDR = 1.0; A3: 66-yr-old woman, CDR = 1.0.

tral and postcentral gyri are adjacent to each other at the central sulcus. The sylvian fissure, separating the superior temporal gyrus from the frontal and parietal gyri, corresponds to the relatively high activity in the superior slices, partially as a result of gyral convolutions around the fissure. The cingulate gyrus, precuneus and cuneus are identifiable in the posterior medial aspect of the brain. Identification of the angular gyrus and supramarginal gyrus is not distinct. Annotations for these areas were approximated from the reference atlases. Separation of the inferior and middle temporal gyri is somewhat difficult because of the orientation of the slice. Distinctions among the superior, middle and inferior occipital gyri were not made as a result of a lack of clear borders. The dentate nuclei are clearly visible in the cerebellum.

In stereotactic coordinates, image sets from three patients with probable Alzheimer's disease revealed a striking anatomic correspondence with the slices in the atlas (Fig. 3). Glucose metabolic activity in the sensorimotor cortex is relatively preserved in Alzheimer's disease (*30*). This relatively small area can be easily and consistently localized in the stereotactic system by comparing it with the PET atlas. The anterior cingulate, striatum, thalamus, visual cortex and cerebellum also show relatively preserved metabolism. Other areas, such as the frontal and parietotemporal association cortices and posterior cingulate gyrus, show decreased glucose metabolism. These regions are defined objectively and reliably in the stereotactic system. Subcortical structures are clearly identifiable, but their locations in Alzheimer's disease are shifted somewhat laterally as a result of cerebral atrophy and ventricular dilation.

DISCUSSION

A stereotactic PET atlas of the brain and examples of its use were presented. By referring to the atlas with knowledge of the characteristics of emission tomographic imaging, consistent anatomic sites of the signals can be identified by means of indirect localization. It was also found that the images obtained by a current state-of-the-art PET system have greatly improved spatial information, enabling direct localization of major structures, especially in the stereotactic coordinates. However, interactions of functional tracer distribution and the underlying anatomy must be recognized and accounted for when interpreting scans (*31*).

A key step for the stereotactic approach is the identification of the intercommissural AC-PC line on PET image sets. The original definition of the intercommissural line was a line passing through the superior edge of the AC and the inferior edge of the PC (*32*). The definition was somewhat modified by different investigators and imaging modalities. When using MRI, a definition of a line passing

through the centers of the two commissures is preferable and is insensitive to size differences of the AC (*20*). However, because the AC and PC are only 25 mm apart in the standard coordinates, this subtle difference in definition might cause a relatively larger difference in the localization of cortical structures. When estimating the intercommissural line on PET images, both Friston et al. (*17*) and Minoshima et al. (*18*) used more than two landmarks and included cortical landmarks. This adaptation may reduce the error caused by using only two subcortical landmarks to define the intercommissural line. They validated their methods based on different definitions of the intercommissural line (center-to-center orientation by Friston et al. and superior-to-inferior edges by Minoshima et al.) and showed a comparable accuracy between the methods. By using either method, stereotactic reorientation can be achieved easily on PET images, facilitating the routine use of this approach in the clinical setting. In fact, the authors have been testing the automated stereotactic alignment procedure as a part of the routine image processing for more than 1 yr and have found great advantages in structural identification when visually interpreting functional brain images.

When applying indirect localization based on the standard coordinate system, normal individual anatomic variations must be known. Talairach et al. (*6*) confirmed a certain amount of individual variation in the bicommissural stereotactic system at the central sulcus, periinsular, sylvian, lower frontal, calcarine, parietooccipital, upper temporal, middle temporal, pericallosal, callosomarginal and cingulate regions. Recent studies, using MRI, also showed variances in the coordinate system at the central sulcus, parietooccipital sulcus, marginal sulcus, sylvian fissure, pre- and postcentral sulcus and calcarine sulcus (*13,14,18*). Hemispheric differences also exist in normal brains (Fig. 2) but were not taken into account in the initial studies. Variations in the size of the temporal speech region (*33*), frontal region (*34*), shape of the sylvian fissure (*14,35*), size and number of the transverse temporal gyri (*36*) and asymmetries at the posterior opercular regions (*37*) were also reported. Observers must know these possible variations and asymmetries on an individual's brain image set when referring to the coordinate system. Cerebral asymmetry can be compensated, to some extent, by using a different standard atlas for each hemisphere, which should be established on a large number of observations. In PET neuronal activation analyses, these variations are compensated for by using a smoothing filter, sacrificing spatial resolution of the image (*38,39*). Some of these structures, e.g., calcarine and sylvian fissure, can be localized on an individual's PET image set by visual inspection, suggesting that individual direct localization following the indirect stereotactic approach enhances the accuracy of localization in some instances. Therefore, direct and indirect localization approaches are not competitive but, rather, complementary.

Limitations of the indirect localization approach obviously arise in subjects who do not have normal brain structure. Cerebral atrophy occurs in demented patients who often are referred for functional imaging evaluation. Fox and Kall (*40*) predicted a reasonable accuracy for the stereotactic approach if enlarged subarachnoid and ventricular spaces were corrected. Nonlinear regional anatomic standardization can be used for this purpose (*27*), although PET signals themselves are affected by thinning of the cortex (*41*) and cannot be corrected by the anatomic standardization. If a subject has a mass lesion in the brain, the indirect localization using individual MRI or CT scans is absolutely necessary. However, the bicommissural stereotactic approach would provide additional information when the presence of cerebral edema inhibits visualization of surrounding structures on anatomic images and when therapeutic interventions through normal structures are performed (*25*).

The merits of using the bicommissural stereotactic approach are objectivity and consistency. Even if target structures are not identifiable in an individual functional image by visual inspection, the stereotactic approach provides the most likely location, based on statistical definition. Therefore, the approach is also suitable for low-resolution imaging modalities. By comparing the atlas and an individual's functional image, brain structures can be localized consistently in the bicommissural stereotactic system. This reference system was proved to be stable and reliable, supporting its routine use in functional brain imaging. In certain cases, the stereotactic approach may obviate the additional cost and patient compliance required saafor anatomic images. The stereotactic coordinates also minimize subjective biases that are inherent in visual inspection alone. The coordinates assigned to various cerebral structures permit cross-modality and cross-institutional comparisons.

A stereotactic brain atlas obtained by PET was presented, and its limitations and applications were discussed. It is concluded that the atlas provides an aid for the visual interpretation of functional brain images and enhances the accuracy of structural identification. The authors expect wider applications of the stereotactic approach, not only in the research setting, but also in routine clinical situations.

ACKNOWLEDGMENTS

The authors thank PET facility staff for isotopic production and the performance of PET studies. This work was supported in part by grants DE-FG02-87-ER60561 from the Department of Energy and RO1-NS24896 from the National Institutes of Health.

APPENDIX

Anatomic Abbreviations Used In Figure 1

The lingual gyrus, precuneus and fusiform gyrus have two different abbreviations because of limited space on the atlas. Subcortical structures, such as the thalamus, caudate nucleus and putamen, are not annotated because of their obvious structures and locations.

C	cingulate gyrus
CBL	cerebellum
Cu	cuneus
d	medial aspect of the frontal lobe
D	dentate nucleus of the cerebellum

F(GF) fusiform gyrus
Ga angular gyrus
GF(F) fusiform gyrus
GFi inferior frontal gyrus
GFm middle frontal gyrus
GFs superior frontal gyrus
GL (L) lingual gyrus
GO orbital gyri
GOc occipital gyrus
GPrC precentral gyrus
GPoC postcentral gyrus
GR rectal gyrus
Gsm supramarginal gyrus
GTi inferior temporal gyrus
GTm middle temporal gyrus
GTs superior temporal gyrus
H parahippocampal (hippocampal) gyrus
L (GL) lingual gyrus
LPi inferior parietal lobule
LPs superior parietal lobule
M extraocular muscles
P (Pcu) precuneus
Pcu (P) precuneus
sc subcallosal gyrus
U uncus

REFERENCES

1. Schoultz TW, Morrison JR, Calhoun JD. Atlas of the human brain for use in diagnosis by computer-assisted tomography. *Surg Neurol* 1976;5:255–266.
2. Matsui T, Kawamoto K, Iwata M, et al. Anatomical and pathological study of the brain by CT scanner—1: anatomical study of normal brain. *Comput Tomogr* 1977;1:3–43.
3. Tokunaga A, Takase M, Otani K. The glabella-inion line as a baseline for CT scanning of the brain. *Neuroradiology* 1977;14:67–71.
4. Van Buren JM, Maccubbin DA. An outline atlas of the human basal ganglia with estimation of anatomical variants. *J Neurosurg* 1962;19:811–839.
5. Kall BA, Kelly PJ, Goerss S, Frieder G. Methodology and clinical experience with computed tomography and a computer-resident stereotactic atlas. *Neurosurgery* 1985;17:400–406.
6. Talairach J, Szikla G, Tournoux P, et al. *Atlas d'anatomie stéréotaxique du télencéphale*. Paris: Masson; 1967.
7. Takase M, Tokunaga A, Otani K, Horie T. Atlas of the human brain for computed tomography based on the glabella-inion line. *Neuroradiology* 1977;14:73–79.
8. Vanier M, Lecours R, Ethier R, et al. Proportional localization system for anatomical interpretation of cerebral computed tomograms. *J Comput Assist Tomogr* 1985;9:715–724.
9. Latchaw RE, Lunsford LD, Kennedy WH. Reformatted imaging to define the intercommissural line for CT-guided stereotaxic functional neurosurgery. *AJNR Am J Neuroradiol* 1985;6:429–433.
10. Villemure JG, Marchand E, Peters T, Leroux G, Olivier A. Magnetic resonance imaging stereotaxy: recognition and utilization of the commissures. *Appl Neurophysiol* 1987;50:57–62.
11. Vanier M, Ethier R, Clark J, et al. Anatomical interpretation of MR scans of the brain. *Magn Reson Med* 1987;4:185–188.
12. Rumeau C, Gouaze A, Salamon G, et al. Identification of cortical sulci and gyri using magnetic resonance imaging: a preliminary study. In: Gouaze A, Salamon G, eds. *Brain anatomy and magnetic resonance imaging*. New York: Springer-Verlag; 1988:11–31.
13. Steinmetz H, Fürst G, Freund HJ. Cerebral cortical localization: application and validation of the proportional grid system in MR imaging. *J Comput Assist Tomogr* 1989;13:10–19.
14. Steinmetz H, Fürst G, Freund HJ. Variation of perisylvian and calcarine anatomic landmarks within stereotaxic proportional coordinates. *Am J Neuroradiol* 1990;11:1123–1130.
15. Fox PT, Perlmutter JS, Raichle ME. A stereotactic method of anatomical localization for positron emission tomography. *J Comput Assist Tomogr* 1985;9:141–153.
16. Fox PT, Mintun MA, Reiman EM, Raichle ME. Enhanced detection of focal brain responses using intersubject averaging and change-distribution analysis of subtracted PET images. *J Cereb Blood Flow Metab* 1988;8:642–653.
17. Friston KJ, Passingham RE, Nutt JG, et al. Localization in PET images: direct fitting of the intercommissural (AC-PC) line. *J Cereb Blood Flow Metab* 1989;9:690–695.
18. Minoshima S, Keoppe RA, Mintun MA, et al. Automated detection of the intercommissural line for stereotactic localization of functional brain images. *J Nucl Med* 1993;34:322–329.
19. Minoshima S, Frey KA, Koeppe RA, et al. Stereotactic metabolic atlas of the brain as a new diagnostic tool for functional brain imaging. *J Nucl Med* 1992;33(suppl):858.
20. Bergvall U, Rumeau C, Bunnen YV, Corbaz JM, Morel M. External references of the bicommissural plane. In: Gouaze A, Salamon G, eds. *Brain anatomy and magnetic resonance imaging*. New York: Springer-Verlag; 1988:2–10.
21. Powers WJ, Perlmutter JS, Videen TO, et al. Blinded clinical evaluation of positron emission tomography for diagnosis of probable Alzheimer's disease. *Neurology* 1992;42:765–770.
22. Holman BL, Johnson KA, Gerada B, Carvalho PA, Satlin A. The scintigraphic appearance of Alzheimer's disease: a prospective study using technetium-99m-HMPAO SPECT. *J Nucl Med* 1992;33:181–185.
23. Wienhard K, Eriksson L, Grootoonk S, et al. Performance evaluation of the positron scanner ECAT EXACT. *J Comput Assist Tomogr* 1992;16:804–813.
24. Minoshima S, Berger KL, Lee KS, Mintun MA. An automated method for rotational correction and centering of three-dimensional functional brain images. *J Nucl Med* 1992;33:1579–1585.
25. Talairach J, Tournoux P. *Co-planar stereotaxic atlas of the human brain*. New York: Thieme; 1988.
26. Pietrzyk U, Herholz K, Heiss WD. Three-dimensional alignment of functional and morphological tomograms. *J Comput Assist Tomogr* 1990;14:51–59.
27. Minoshima S, Koeppe RA, Frey KA, Kuhl DE. Anatomical standardization: linear scaling and non-linear warping of functional brain images. *J Nucl Med* 1994: in press.
28. Salamon G, Huang YP. *Radiologic anatomy of the brain*. New York: Springer-Verlag; 1976.
29. Ono M, Kubik S, Abernathey CD. *Atlas of the cerebral sulci*. New York: Thieme; 1990.
30. Kuhl DE, Metter EJ, Riege WH. Patterns of cerebral glucose utilization in depression, multiple infarct dementia, and Alzheimer's disease. *Res Publ Assoc Res Nerv Ment Dis* 1985;63:211–226.
31. Mazziotta JC, Koslow SH. Assessment of goals and obstacles in data acquisition and analysis from emission tomography: report of a series of international workshops. *J Cereb Blood Flow Metab* 1987;7(suppl):S1–S3.
32. Talairach J, De Ajuriaguerra J, David M. Études stéréotaxiques des structures encéphaliques profondes chez l'homme. *Presse Med* 1952;28:605–609.
33. Geschwind N, Levitsky W. Human brain: left-right asymmetries in temporal speech region. *Science* 1968;161:186–187.
34. Orthner H, Sendler W. Planimetrishce Volumetrie an menschlichen Gehirnen. *Fortschr Neurol Psychiatr* 1975;43:191–209.
35. Rubens AB, Mahowald MW, Hutton JT. Asymmetry of the lateral (sylvian) fissures in man. *Neurology* 1976;26:620–624.
36. Galaburda AM, LeMay M, Kemper TL, Geschwind N. Right-left asymmetries in the brain. *Science* 1978;199:852–856.
37. Kertesz A, Black SE, Polk M, Howell J. Cerebral asymmetries on magnetic resonance imaging. *Cortex* 1986;22:117–127.
38. Friston KJ, Frith CD, Liddle PF, Frackowiak RSJ. Comparing functional (PET) images: the assessment of significant change. *J Cereb Blood Flow Metab* 1991;11:690–699.
39. Worsley KJ, Evans AC, Marrett S, Neelin P. A three-dimensional statistical analysis for CBF activation studies in human brain. *J Cereb Blood Flow Metab* 1992;12:900–918.
40. Fox PT, Kall B. Stereotaxy as a means of anatomical localization in physiological brain images: proposals for further validation. *J Cereb Blood Flow Metab* 1987;7(suppl):S18–S20.
41. Müller-Gärtner HW, Links JM, Prince JL, et al. Measurement of radiotracer concentration in brain gray matter using positron emission tomography: MRI-based correction for partial volume effects. *J Cereb Blood Flow Metab* 1992;12:571–583.